

Development of Low-Exergy-Loss, High-Efficiency Chemical Engines

Investigators

C. F. Edwards, Associate Professor, Mechanical Engineering; Kwee-Yan Teh, Shannon L. Miller, Graduate Researchers

Introduction

The objective of this project is to construct a device that demonstrates the feasibility of combustion with significantly reduced irreversibilities. Reducing the entropy generation during combustion so as to increase thermal efficiency is an approach applicable to all internal combustion engines and therefore has the potential to significantly reduce greenhouse gas emissions.

Today's simple-cycle engines have first-law efficiencies (work per unit LHV) less than 50% due to exergy destruction during combustion, heat transfer losses, and poor extraction (high exhaust enthalpy). The goal of this project is to reduce these losses using an extreme compression/expansion approach so as to achieve simple-cycle, first-law efficiencies well beyond 50%.

Background

Any unrestrained reaction (combustion) engine involves the transformation of reactants from a chemically frozen state of non-equilibrium to products that closely approach (with minor exceptions) a state of complete thermo-chemical equilibrium. These chemically frozen reactants and equilibrated products can each be represented thermodynamically by surfaces in the U, S, V space. Each point on the surface represents a state that can be reached from any other state by a series of reversible processes governed by the Fundamental Relation. Jumping from one surface (the reactant surface) to a different surface (the product surface) involves an irreversible process resulting in entropy generation. Figure 1, part *a*, shows the surface for the frozen reactants (stoichiometric propane/air) in blue and the equilibrated products (including full dissociation) in red.

Also shown in the figure is the trajectory of an ideal, reactive Otto cycle (a fuel-air cycle) in black. The resource (reactant mixture) begins at ambient conditions (300 K, 1 atm) on the blue surface and is adiabatically and reversibly compressed to a reduced volume. Since this process is reversible (no entropy generation), the line lies on the blue surface. At the end of the compression process, chemical reaction is permitted, releasing the resource from its chemically frozen state and transforming it to equilibrium products. For the ideal cycle shown, this reaction is depicted by the dashed line moving from the blue to the red surface at constant U and V , but with S increasing due to entropy generation. This entropy generation is the irreversibility inherent in an unrestrained reaction. The exergy destroyed in this process is given by the Gouy-Stodola theorem as the product of the entropy generated and the temperature of the surroundings, such that the total exergy destruction due to combustion is

$$X_{\text{destroyed by combustion}} = \int \delta X_{\text{destroyed}} = \int T_0 \delta S_{\text{generated}} = T_0 S_{\text{generated by combustion}} \quad (1)$$

This destroyed exergy is no longer available to do work. The efficiency potential of the system is decreased due to this entropy production.

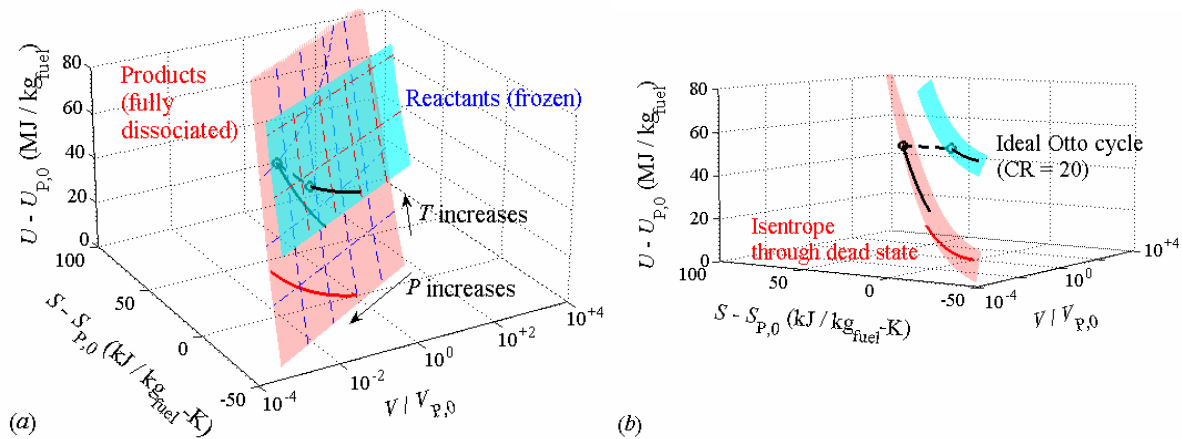


Figure 1: Internal energy/entropy/volume thermodynamic surfaces for stoichiometric propane/air. *a*) Dashed lines indicate isobars at 0.1, 1, 10 and 100 bar, isotherms at 1000 and 2000 K for reactants, and isotherms at 1000, 2000 and 3000 K for products. *b*) These same surfaces are shown in a view rotated to emphasize entropy generation. The ideal, reactive Otto cycle is depicted by the black lines while an isentrope with products expanded to the thermal dead state ($T_0 = 300$ K, $P_0 = 1$ atm) is shown in red.

In Part *b*, the reactant and product surfaces are rotated to emphasize the entropy generated due to reaction. This view also shows more clearly the completion of the Otto cycle by expanding the product gases along an adiabatic/reversible trajectory through the same volume ratio used for compression. Note that upon completion of the cycle a significant amount of internal energy is still retained in the working fluid. An ideal expansion isentrope for the work extraction process would be one that expands to the product thermal dead state ($T_0 = 300$ K, $P_0 = 1$ atm), as shown by the red curve on the product surface. Comparison of the Otto-cycle expansion process with this ideal isentrope emphasizes how poorly matched conventional gas expansion processes are with stoichiometric combustion. Even if expansion to atmospheric pressure is used (the ideal, reactive Atkinson cycle), the mismatch between trajectories indicates that a serious problem exists with respect to work extraction.

The key message from these figures is that combustion irreversibility can be reduced by moving the reactant conditions (U, V state) to conditions with higher internal energy where the distance between the reactant and product surfaces along the entropy axis is reduced. Reducing this distance reduces the entropy generated during combustion. Figure 2 shows a two dimensional view of the U - S axes. Points *A, B, C*, and *D* define a standard Otto cycle with a 10:1 compression ratio. As the compression ratio is increased (up to 200:1 in the diagram), the constant volume lines for the products and reactants approach each other and the entropy generation for the cycle decreases.

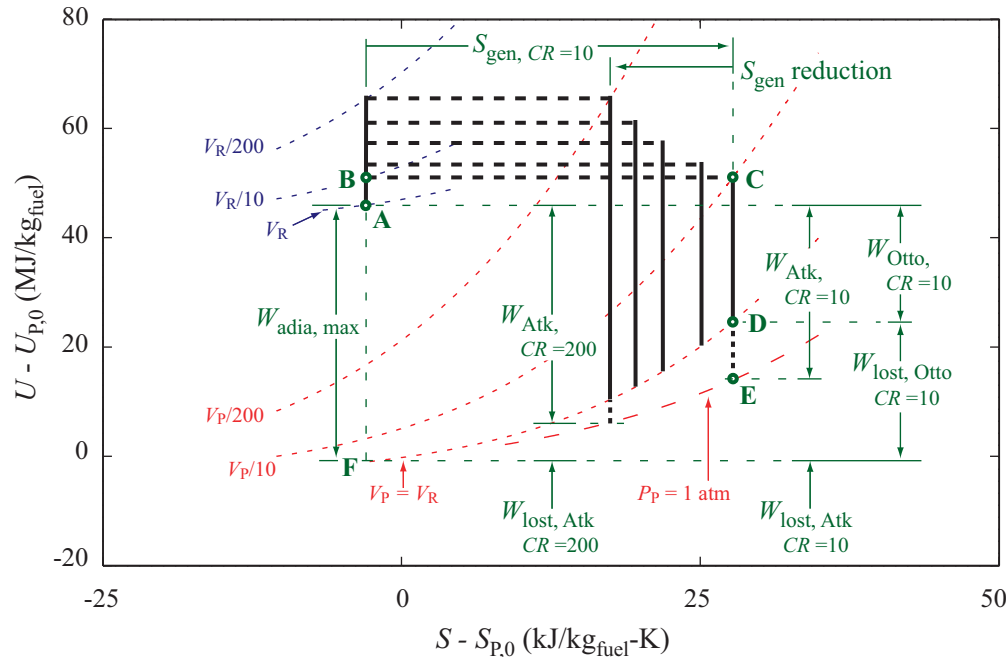


Figure 2: Ideal Otto and Atkinson cycles for stoichiometric propane/air on a U - S diagram. Compression ratios shown include 10, 20, 50, 100, and 200:1. At a compression ratio of 200:1, the work lost due to combustion irreversibility can be reduced to one-half that from the 10:1 compression ratio case.

Another benefit of moving to higher compression ratios can be seen by looking at the internal energy of the exhaust. At point D (after a CR of only 10:1), there is still significant internal energy remaining in the system. One way to transfer more of the resource's exergy to work is to use an Atkinson cycle and expand the products to atmospheric pressure (to point E). Another way is to move to higher compression ratios. As compression ratio increases, the post-combustion products are better positioned for extraction; they are closer to the ideal isentrope shown in Figure 1. The exhaust state is much closer to the thermomechanical dead state, or the state of the environment (point F).

Figure 3 summarizes the results that can be obtained from extreme compression, showing the theoretical first-law efficiencies obtainable using extreme compression in both an adiabatic, ideally expanded (Atkinson) engine and an adiabatic, symmetric compression/expansion (Otto) engine. The red and blue colored bands represent 70-80% of the first law efficiencies which is often what engines achieve in practice, after implementation efficiencies have been included. Also shown on the graph are two real engine data points representing two simple-cycle, symmetric compression/expansion engines (data from Heywood, 1988).

Near compression ratios of 100:1, the bands representing 70-80% of the ideal, first-law efficiencies surpass 50%. The goal of this project is to determine the feasibility of building an engine with compression ratios of 100:1 and greater. By building an extreme compression/expansion device, we can explore the performance possibilities of an engine operating in this regime. Proving the feasibility of higher efficiencies at extreme

compression ratios is the first step to designing new engines with significantly improved efficiency.

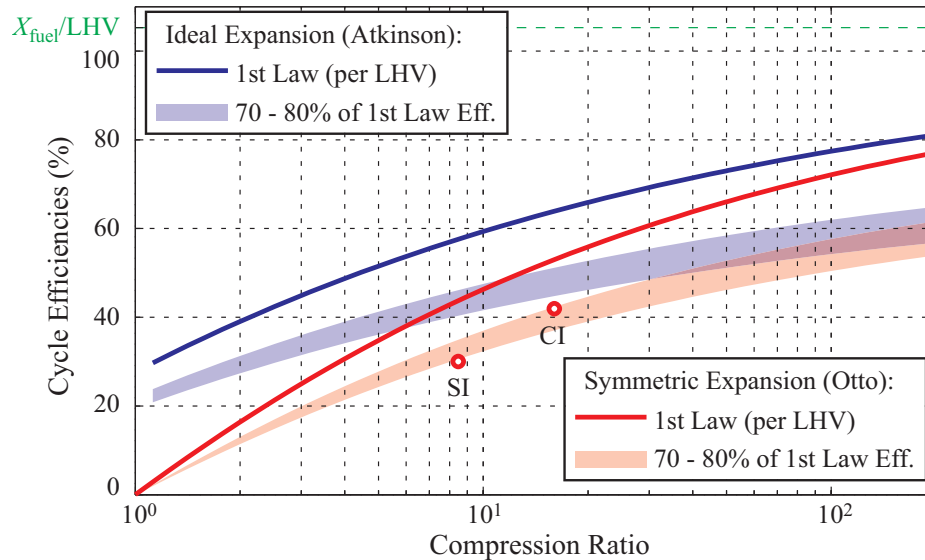


Figure 3: First law efficiencies vs. compression ratio for stoichiometric propane/air. As compression ratio increases, S_{gen} decreases and more exergy is transferred to work during expansion. As such, the Atkinson-cycle and Otto-cycle efficiencies begin to converge. The red and blue bands represent 70-80% of the first law efficiencies, which is representative of what current engines often achieve in practice after implementation efficiencies are included.

Results

As of this report, we are four months into the project. We have spent these initial months designing the extreme compression/expansion machine as well as defining the first prototype experiment which will be used to characterize particularly challenging components of the design.

Design Concept

The purpose of the extreme compression/expansion machine is to examine engine process efficiencies at very high compression ratios and speeds. Figure 4 shows a basic concept drawing of the device. High-pressure gas drives two pistons toward each other at high speed, compressing air in between them. Fuel injection and combustion occur in the center section, driving the pistons back toward their original positions. Two free pistons are used to avoid the reaction forces associated with the high peak pressures required. The machine will conduct just one cycle of compression, combustion, and expansion and will operate with compression ratios in excess of 100:1.

These high compression ratios lead to high, post-combustion temperatures— ~ 3300 K for stoichiometric conditions. High temperatures in turn result in increased heat transfer, often dominating potential efficiency gains due to reduced irreversibility. For this reason, the compression/expansion process is conducted an order of magnitude faster than in a conventional engine. Our current goal is to realize piston speeds near Mach 0.3 (~ 150 m/s) in the reactant gases. This Mach number was chosen to provide an order of

magnitude decrease in the time available for heat transfer while still avoiding flow compressibility effects. To avoid enhanced losses due to poor surface-to-volume ratio, the apparatus is designed to have unit aspect ratio at TDC.

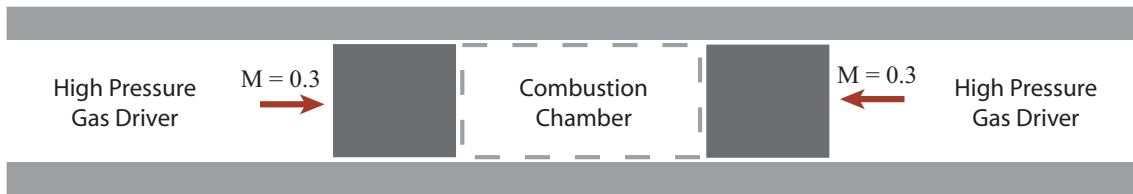


Figure 4: Basic concept of the extreme compression/expansion device. Two pistons are driven toward each other at high speed during the compression stroke. Fuel injection, autoignition, and combustion occur in the center region, driving each piston back toward its original position at high speed.

Figure 5 shows a concept schematic that includes our basic approach for driving the pistons and sensing their positions. The working pistons in the main cylinder are connected to a high-pressure gas reservoir by large-area, fast-opening poppet valves. When the valves open, the high-pressure gas from the reservoir drives the pistons toward each other at high speed. Each poppet valve is initially held closed (against reservoir pressure) by a small piston attached to the end of its valve stem (shown in green in Fig. 5). A fast-acting, solenoid valve vents a small, high-pressure volume, allowing the piston to move and the poppet valve to open. Although we have depicted the system using two poppet-valve actuators, designs using a single actuator with downstream flow splitting have also been considered.

Our basic concept for piston position sensing is also shown in the figure. By constructing the cylinder of austenitic stainless steel and the piston of ferritic steel, we can magnetically sense the piston position through the cylinder wall without penetrating the interior surface of the cylinder. We have tested and evaluated several types of magnetic sensors including inductive sensors, magnetoresistive sensors, and Hall effect sensors. The inductive sensors have proven to be very effective—sensing a moving, ferritic object that is smaller than our piston through a half-inch-thick austenitic stainless steel wall. These sensors will be mounted in holes that pass partially through the cylinder wall, maintaining both the cylinder's structural integrity under high pressures and the surface finish for the sealing rings. Near TDC where piston velocities are small and position resolution requirements are high, it may be necessary to use a LVDT approach to sensing piston position. A combination of prototype experiments and modeling will determine whether this technique is required.

While piston rings are not depicted in the conceptual schematic, they are a critical component of the design. Most standard piston rings are rated for much lower pressures and speeds than are required for this application. The prototype, whose goals are discussed in the next section, will be used to test several ring options to determine the best combination for control of gas leakage and ring friction. These options include standard piston rings with oil lubrication, fluorocarbon rings without lubrication, and use of a bearing surface with a small clearance and sufficiently high leakage-flow pressure loss that no sealing mechanism is required.

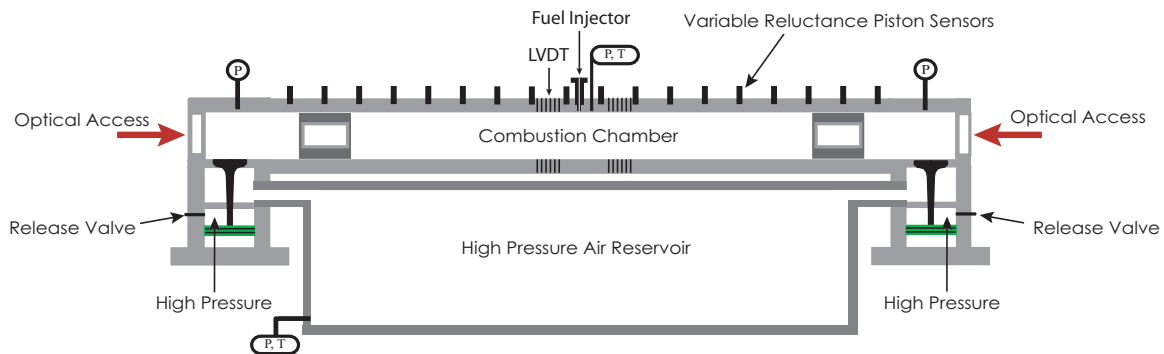


Figure 5: Conceptual schematic of compression/expansion device with two free pistons.

Modeling

In order to understand the various design choices, we calculated the reservoir pressures and valve sizes required to achieve the desired compression ratios and speeds for our conceptual design. The following figures assume a poppet valve head diameter of 50 mm with an 8 mm lift. To establish limiting performance, the valve is assumed to open instantaneously. Figure 6 shows the reservoir pressures required for pistons of three masses to achieve particular compression ratios. The nominal mass (6.3 kg) was chosen by assuming a steel piston of unit aspect ratio (100 mm diameter and length). The other masses are perturbations about this value. These results also assume a reservoir size of 0.18 m^3 corresponding to the use of a 24-cm diameter cylinder that is 4 m in length.

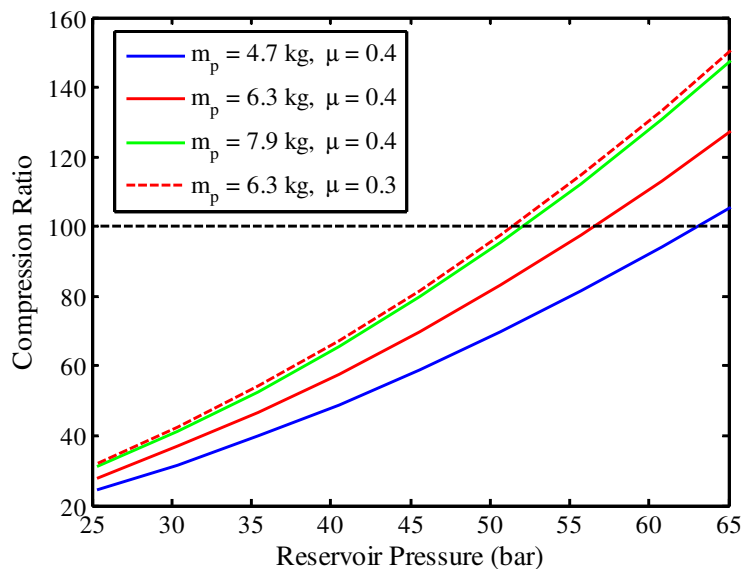


Figure 6: Achievable compression ratio as a function of initial reservoir pressure for three piston masses.

The figure shows that, because they store less kinetic energy, lighter pistons require higher initial reservoir pressures to achieve the same peak compression ratio. In this figure, friction was modeled assuming the use of two, 10 mm-wide rings with a friction coefficient of 0.4 (twice the value of a standard PEEK ring on steel). Reduction of the

friction coefficient to 0.3, while keeping piston mass fixed, lowers the initial reservoir pressure required to achieve a particular compression ratio.

Figure 7 shows the mean piston speed (total compression distance divided by total compression time) achieved using the same valve model and reservoir pressures. The mean piston speeds achieved for a compression ratio of 100:1 are close to the Mach 0.3 goal (~ 100 m/s at 300 K). Peak speeds are ~ 1.5 times mean piston speed. A lower piston mass will have higher mean speeds for the same reservoir pressure, but will have a lower final compression ratio. By varying piston mass, reservoir pressure, and valve area, we can achieve the desired compression ratios with the required piston speeds.

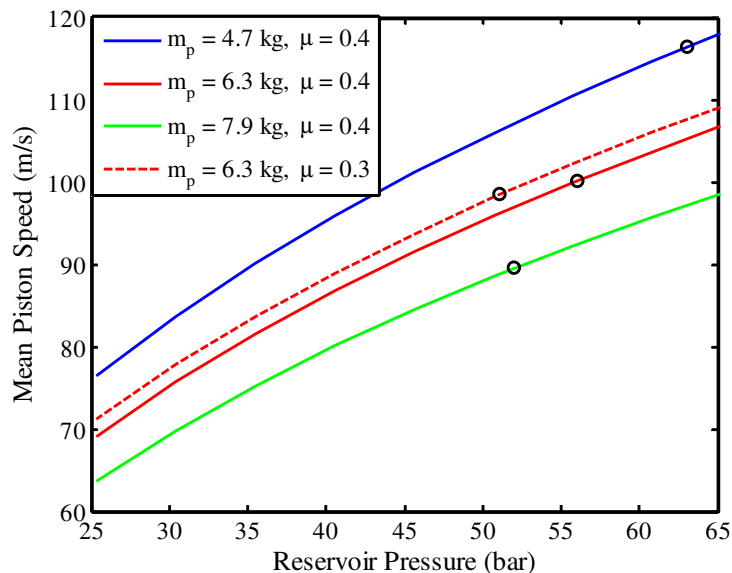


Figure 7: Mean piston speed as a function of initial reservoir pressure. The circles show the mean piston speed for the reservoir pressure that is associated with a 100:1 compression ratio based on Fig. 6.

Figure 8 shows a simulation of the system dynamics (without combustion) for the previously defined model parameters and the unit aspect ratio piston. Parts *a* and *b* illustrate the piston position and velocity profiles respectively. While the simulation demonstrates the motion for a single piston, the results are readily applicable to a two-piston system. After the initial compression/expansion profile, the piston continues to oscillate until the system has equilibrated. The poppet valve will remain open for the duration of the experiment, allowing air to move freely between the reservoir and the cylinder. Upon reaching equilibrium, we will depressurize the cylinder, reset the valve and piston to their original positions, and repeat the experiment. Figure 8, part *c*, shows the mass of air in the driver section of the cylinder as a function of time. The different slopes correspond to choked and unchoked flow across the poppet valve and can be linked to the pressure profiles in Fig. 8, part *d*. When the cylinder driver pressure is less than $\sim 50\%$ of the reservoir pressure, the flow across the poppet valve is choked, leading to the maximum flow rate for a given reservoir pressure.

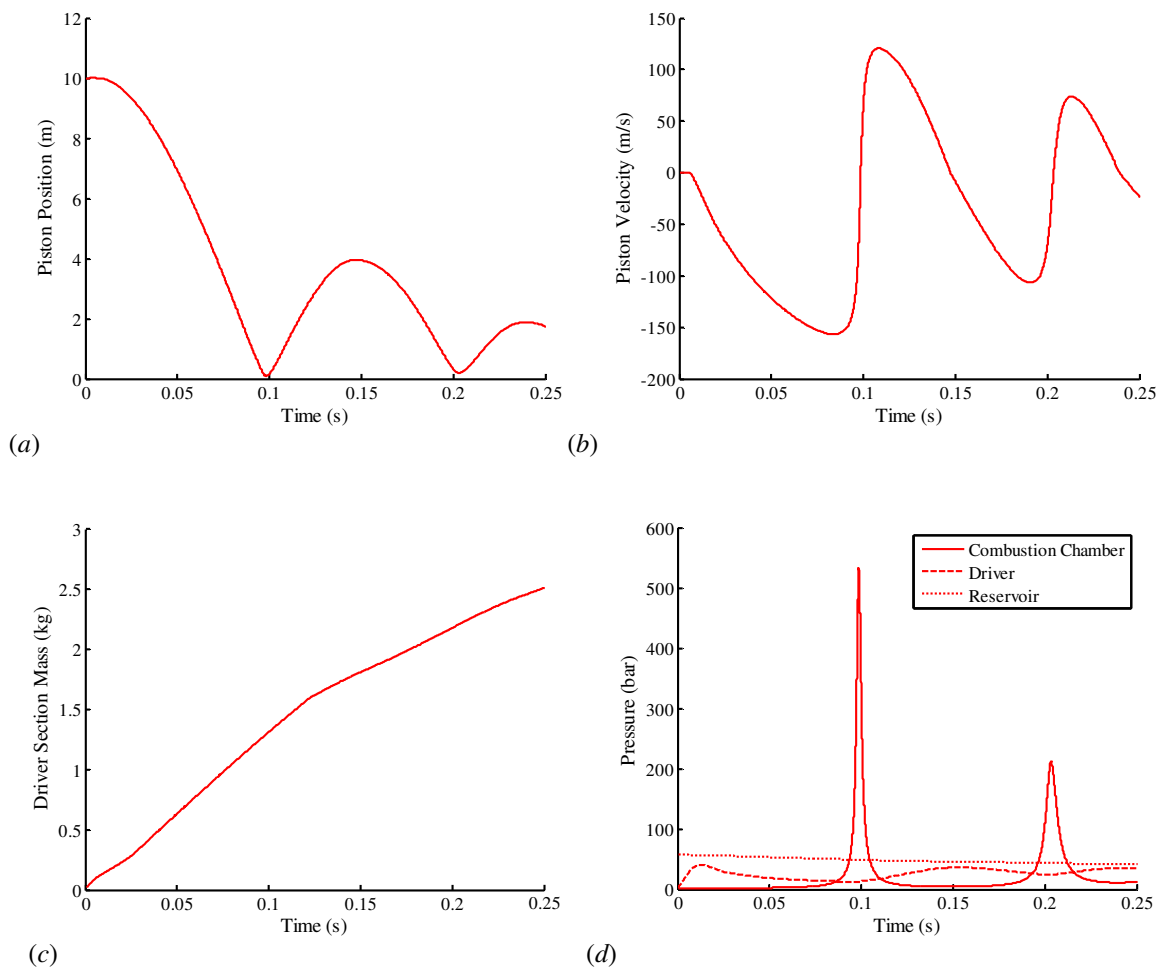


Figure 8: Dynamic simulation results for a single-piston system with a 6.3 kg piston and 56 bar, 0.18 m³ gas reservoir. *a)* piston position *b)* piston velocity *c)* mass of air in the driver section and *d)* pressures as a function of time.

The Prototype

The goal of the prototype is to provide an experimental apparatus for resolving some of the key technical challenges before designing the larger machine. These key challenges include:

- Valve mechanism repeatability
- Piston position sensing accuracy
- Sealing ring design and performance
- Achievable system dynamics and performance

These issues will be addressed in a prototype that is similar in design to the actual system, but using only a single piston and not including combustion. The prototype will be constructed with a smaller bore (50 mm diameter) and will be designed for compression ratios up to 50:1 (peak pressures near 200 bar). Significantly lower forces,

due to lower compression ratios and no combustion, allow the prototype to be built with a single piston. A poppet-valve compressed-air mechanism for driving the piston, a magnetic piston sensing system, and various sealing ring options will be tested. The prototype testing will be used to characterize these systems for incorporation into the final design.

Contact

C.F. Edwards: cfe@stanford.edu